Spectrochimica Acta Part A: Molecular and Biomolecular Spectroscopy 247 (2021) 119072

Contents lists available at ScienceDirect

Spectrochimica Acta Part A: Molecular and Biomolecular Spectroscopy

journal homepage: www.elsevier.com/locate/saa

A modular template for the design of thiol-triggered sensors and prodrugs

Jessica Renee Knight [a], Yingying Wang [a], Shi Xu [b], Wei Chen [a], Clifford E. Berkman [a], Ming Xian [b,*]

[a] Department of Chemistry, Washington State University, Pullman, WA 99164, USA
[b] Department of Chemistry, Brown University, Providence, RI 02912, USA

ARTICLE INFO

Article history:
Received 24 September 2020
Received in revised form 6 October 2020
Accepted 7 October 2020
Available online 13 October 2020

Keywords:
Fluorescent probe
Prodrug
Biothiols
Sulfinic acid

ABSTRACT

A unique reaction between thiols (RSH) and alkyl sulfonylbenzothiazole was discovered. This reaction was specific for thiols and produced a sulfinic acid (RSO_2H) as the intermediate, which further triggered an intramolecular cyclization to release a -OH containing payload. This reaction was used to develop thiol-triggered fluorescent sensors and prodrugs. The modular design of this template provides tunability of the release profiles of the payloads.

1. Introduction

Biothiols include both small molecule compounds (such as cysteine-Cys, homocysteine-Hcy, and glutathione-GSH) and protein bound cysteine residues. These –SH containing species play crucial roles in biological systems, especially in maintaining cellular redox homeostasis via –SH based redox reactions to form a variety of thio-derivatives (such as disulfides, *S*-nitrosothiols, and sulfenic acids) [1–3]. Abnormal levels of biothiols are known to be associated with many diseases such as AIDS, cardiovascular diseases, and neurodegenerative diseases [4–6]. In addition, various types of cancer have elevated levels of biothiols, especially GSH. This elevated level of GSH impacts apoptotic resistance and drug resistance in cancer cells [7–11].

Due to the importance of thiols in biology, many reactions and reagents have been developed to specifically label or sense thiol residues [12–17]. These reactions/reagents normally take the advantage of much stronger nucleophilicity of thiols (-SH) than other functional groups (such as amines or hydroxyls) under physiological conditions. Among these reactions/reagents, iodoacetamide (IAM), *N*-ethylmaleimide (NEM), and their derivatives are perhaps most well-known (Scheme 1a). These reagents react with thiols very rapidly and in high yields and have been used as standard protocols for blocking cellular thiols. However, these reagents are not without limitations. For example, recent studies have revealed cross reactivity of IAM/NEM with other cellular thiol-adducts such as sulfenic acids (-SOH) [18–19]. In the search for more specific thiol-blocking reagents, we have discovered several heterocyclic thiosulfonate reagents which showed high reactivity and specificity for thiols. Most importantly they do not show cross reactivity with sulfenic acids [19,20]. These compounds, for instance, methylsulfonylbenzothiazole (MSBT, shown in Scheme 1b), have been used in the labeling of cellular thiol (-SH) and the development of thiol-specific sensors [21]. A unique feature of MSBT is that its reaction with thiols not only produces the desired labeling product (e.g. thio-benzothiazole) but also produces a sulfinic acid (RSO_2H) as the byproduct. This is different from the reactions of IAM or NEM, which just produce the corresponding thiol-adducts. We envisioned the reaction of MSBT could be advantageous as RSO_2H is a potentially reactive functional group under physiological conditions. The formation of RSO_2H could allow us to develop thiol-triggered tandem reactions or modular templates for the design of thiol-sensitive sensors or prodrugs. Herein we would like to report our progress in this attempt.

2. Experimental section

2.1. Materials and instruments

All solvents were reagent grade. Reactions were magnetically stirred and monitored by thin layer chromatography (TLC) with 0.25 mm precoated silica gel plates. Flash chromatography was performed with silica gel 60 (particle size 0.040–0.062 mm). Yields refer to chromatographically and spectroscopically pure compounds, unless otherwise stated. Proton and carbon-13 NMR spectra were recorded on a 400 MHz spectrometer. The solvent for NMR measurements were $CDCl_3$ or DMSO-d_6.

* Corresponding author.
E-mail address: ming_xian@brown.edu (M. Xian).

https://doi.org/10.1016/j.saa.2020.119072
1386-1425/

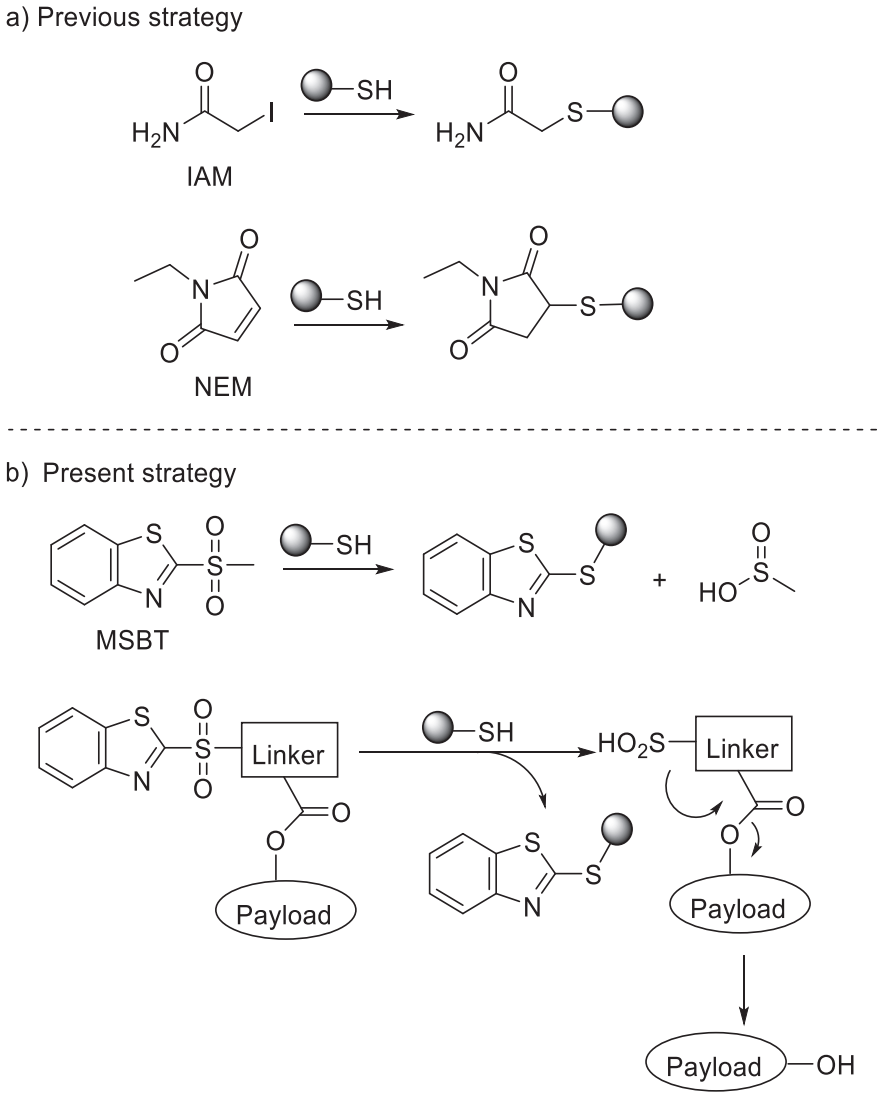

Scheme 1. The design strategy of thiol-labeling reagents.

Fluorescence measurements were taken using a Fluostar Omega Microplate Reader running Omega software version 1.02 and Mars Data Analysis Software Program version 1.10 or on Cary Eclipse fluorescence spectrophotometer.

2.2. Synthesis of SBTP-1, SBTP-2, and SBTP-NO

Compound 1 was prepared from methylsulfonylbenzothiazole (MSBT) and thiosalicylic acid following the known procedure in 80% yield.

Compound 2 was obtained as an off-white solid in quantitative yield. Compound **1** was dissolved in acetonitrile in a round bottom flask. In a separate flask Oxone was dissolved in PBS buffer (50 mM, pH 7.4). The oxone solution was slowly added to the solution of compound **1**. The reaction stirred at rt. for 5 h. The product was extracted with ethyl acetate and dried over $MgSO_4$ and concentrated. It was used for next step without further purification.

SBTP-1 was obtained as a white solid in 76% yield (38 mg). Compound **2** (0.043 g, 0.125 mmol) was dissolved in 1.0 mL of acetonitrile in an oven dried 25 mL round bottom flask. Then DCC (0.044 g, 0.213 mmol) and DMAP (0.001 g, 0.008 mmol) was added to the flask. The flask was placed under argon and allowed to stir for 10 min. Fluorescein (0.018 g, 0.05 mmol) was then added to the reaction flask. The reaction was stirred under argon for 18 h. The reaction was then worked up with water and ethyl acetate. The product was purified column chromatography. ^{1}H NMR (400 MHz, $CDCl_3$) δ 8.55(m, 2H), 8.07 (t, J = 7.2, 2H), 7.98 (d, J = 8.9, 1H), 7.95–7.83(m, 8H), 7.71(dt, J = 26.3,7.6 3H), 7.48–7.58 (m, 4H) 7.24 (s, 2H), 6.98 (dd, J = 8.7, 2.6, 2H), 6.88 (dd, J = 8.7, 2.8, 2H); ^{13}C (100 MHz, $CDCl_3$) δ167.23, 164.42, 152.28, 151.70, 151.67, 136.87,136.58, 135.35, 134.65, 132.34, 132.11, 130.31, 129.13, 128.08, 127.87, 127.69, 127.40, 126.15, 125.40, 125.30, 122.37, 122.31, 117.70, 117.06, 110.54, 42.40; MS(ESI) $[M + H]^+$ calculated $C_{48}H_{27}N_2O_{11}S_4$ 935.05, found $[M + H]^+$ 935.0.

Compound 3 was obtained in quantitative yield as an off-white solid. 2-Marcaptobenzothiazol (670 mg) was dissolved in THF (10 mL), potassium carbonate (1.1 g) was added, and the reaction was stirred for 10 min under argon. Then 3-bromoproponic acid (910 mg) was added. The reaction was allowed to stir overnight at room temperature under argon. The reaction was neutralized with 2 M HCl and the product was extracted with DCM.

Compound 4 was obtained in quantitative yield following the same procedure as compound **2**. ^{1}H NMR (400 MHz, $CDCl_3$) δ 8.22 (d, J = 8.0, 1H), 8.03 (d, J = 8.5, 1H), 7.57–7.68 (m, 2H), 3.83 (t, J = 7.5, 2H), 3.01 (t,

$J = 7.5$, 2H); ^{13}C (100 MHz, $CDCl_3$) δ 164.93, 152.56, 136.76, 128.28, 127.82, 125.57, 122.39, 49.95, 27.45; MS (ESI) $[M + Na]^+$ calculated $C_{10}H_9NNaO_4S_2$ 293.99, found $[M + Na]^+$ 294.0.

SBTP-2 was obtained in 67% yield (67 mg). Compound **4** (54 mg) was added to a dry 25 mL round bottom flask and placed under argon. 5 mL of dry CH_2Cl_2 was added followed by oxalyl chloride (25 μL). Then DMF (0.5 mL) was added dropwise. When the reaction was completed the mixture was concentrated under vacuum. The product was dissolved in dry CH_2Cl_2 (5 mL) under argon. Then fluorescein (20 mg) was added followed by TEA (20 μL). After the reaction was completed the mixture was purified by flash column chromatography to afford 67 mg SBTP-2. ^{1}H NMR (400 MHz, $CDCl_3$) δ 8.19–8.12 (m, 2H), 8.13–8.06 (m, 2H), 8.05–7.99 (m, 2H), 7.65–7.57 (m, 4H), 7.40–7.34 (m, 2H), 7.27 (t, $J = 0.8$ Hz, 2H), 7.27 (s, 2H), 7.26–7.23 (m, 2H), 4.06 (t, $J = 7.0$ Hz, 4H), 3.78 (t, $J = 6.9$ Hz, 4H)·^{13}C (100 MHz, $CDCl_3$) δ 182.63, 174.49, 169.20, 161.87, 155.86, 149.64, 128.16, 127.71, 127.21, 125.91, 125.55, 122.36, 122.07, 121.14, 117.81, 114.44, 106.25, 77.21, 49.83, 29.70. MS (ESI) $[M + H]^+$ Calculated $C_{40}H_{27}N_2O_{11}S_4$ 839.05, found $[M + H]^+$ 839.0.

Compound 10 was prepared in 76% yield as a white solid. Compound **9** (50 mg) and carbon tetrabromide (60 mg) were added to an oven dried round bottom flask and placed under argon. 1 mL of dry CH_2Cl_2 was then added and the flack was placed in an ice bath. In a separate oven dried flask triphenylphosphine (68 mg) was dissolved in 1 mL of dry CH_2Cl_2 then slowly added to the reaction. After stirring overnight, the solvent was removed, and the product was purified by flash column chromatography to yield 38 mg product.

SBTP-NO was obtained as yellow solid in 65% yield. Compound **10** (38 mg) and compound **11** (11 mg) were added to an oven dried round bottom flask. The flask was sealed and backfilled with argon. Then dry DMF (1 mL) was added and the reaction was placed on an ice bath. Then potassium iodide was added. After stirring overnight under argon, the reaction was quenched with water and the product was extracted with ethyl acetate. After purification by flash column chromatography the reaction yielded 32 mg product. ^{1}H NMR (400 MHz, $CDCl_3$) δ 8.55 (dd, 1H), 8.08 (d, $J = 7.5$ Hz, 1H), 7.90 (d, $J = 6.4$ Hz, 2H), 7.87–7.80 (m, 2H), 7.58–7.47 (m, 2H), 7.44 (d, $J = 8.5$ Hz, 2H), 7.23 (d, $J = 8.5$ Hz, 2H), 5.18 (s, 2H), 3.53 (p, $J = 3.5$ Hz, 4H), 1.94 (p, $J = 3.5$ Hz, 4H). ^{13}C NMR (100 MHz, $CDCl_3$) δ 167.44, 164.81, 152.27, 150.39, 136.80, 136.61, 134.64, 134.25, 132.77, 132.32, 131.95, 130.36, 129.97, 127.77, 127.31, 125.30, 122.26, 121.57, 74.45, 50.91, 22.81. MS (ESI) $[M + Na]^+$ Calculated $C_{25}H_{22}N_4NaO_6S_2$ 561.09, found $[M + Na]^+$ 561.0.

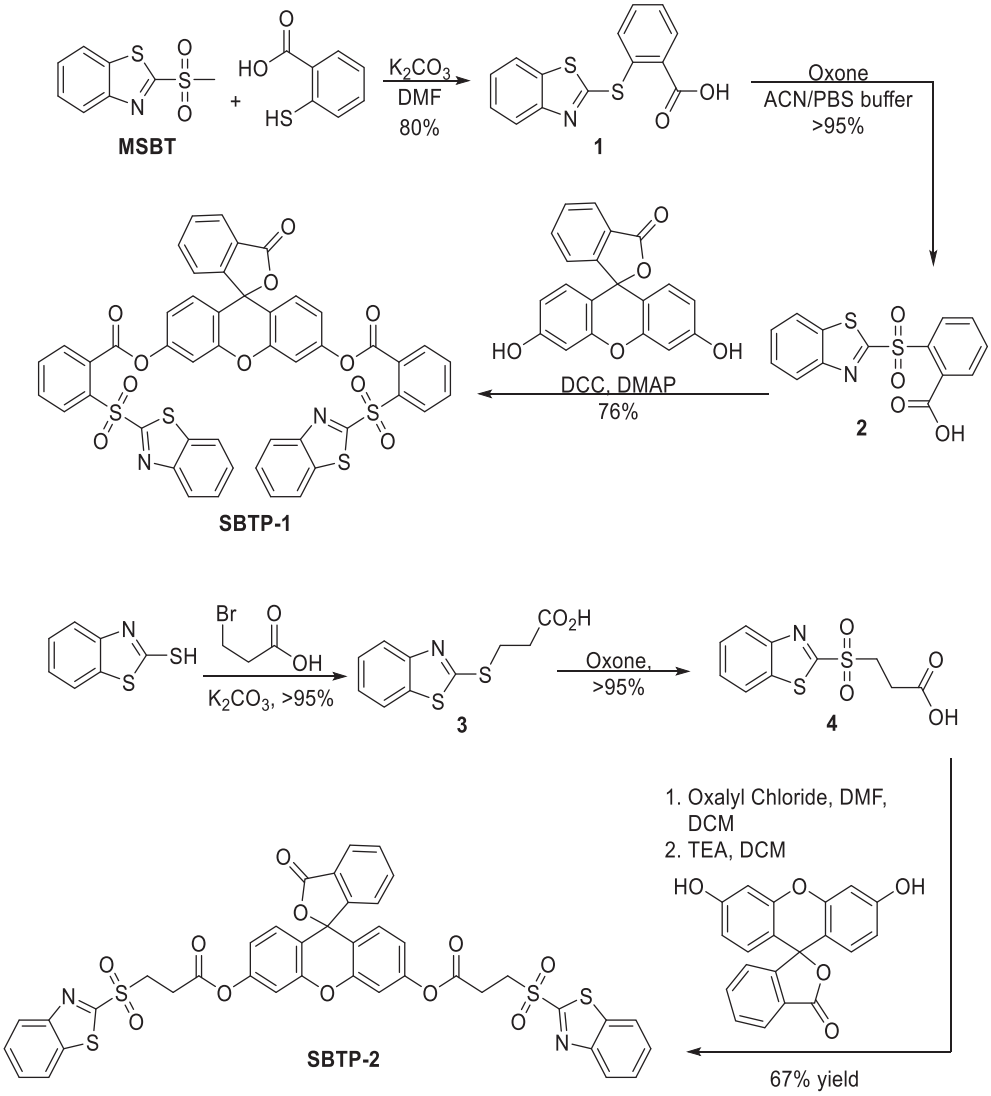

Scheme 2. Synthesis of SBTP-1 and SBTP-2.

2.3. Fluorescence measurements in PBS buffer

All of the measurements were carried out at 37 °C for 60 min in 10 mM PBS buffer (pH 7.4) containing 50% DMSO according to the following procedure: in a test tube, 1.8 mL of 10 mM PBS buffer (pH 7.4) and 1.8 mL DMSO were mixed. A 200 μL of the probe stock solution (0.2 mM) was then added to the mixture. The resulting solution was well-mixed, followed by the addition of the requisite volume of testing species solution. The final volume of the solution was adjusted to 4 mL with 10 mM PBS buffer (pH 7.4). After mixing and standing for 60 min at 37 °C, a 100 μL portion of the reaction solution was loaded onto a 96 well plate to measure fluorescence with $\lambda_{ex/em}$ = 485/520 nm. Error bars represent the standard deviation from triplicate experiments.

2.4. Fluorescence detection in plasma

3 mL of commercially available fetal bovine serum (FBS) was deproteined by adding 6 mL cold pure ethanol and then centrifuging for 30 min. The supernatant was then decanted and used for testing. 1 mL samples were prepared in a test tube. 400 μL deproteinized FBS was added followed by 400 μL DMSO. Then 20 μL of 0.5 mM stock solution of SBTP-1 and 80 μL DMSO was added, followed by the addition of the requisite volume of testing species solution. The final volume of the solution was adjusted to 1 mL with deproteinized FBS. After the samples were incubated at 37 °C for 60 min. 100 μL of each sample were loaded on a 96 well plate and the fluorescence emission were recorded ($\lambda_{ex/em}$ = 485/520 nm). Error bars represent the standard deviation from triplicate experiments.

3. Results and discussion

3.1. Probe synthesis and design

Our idea of the modular template is shown in Scheme 1b. We expected that a hydroxyl containing payload could be tethered with the thiol-reacting site (sulfonylbenzothiazole) via an ester linker. Upon the reaction with thiols the sulfinic acid group would be formed, which should undergo an intramolecular cyclization with the ester group to release the payload. This modular design allows easy modifying all three components: the heterocycle part, the linker, and the payload.

To test this idea, we first employed benzoic acid as the linker and fluorescein as the payload. Fluorescein was chosen because of its excellent fluorescent property and stability in esters. More importantly the hydroxyl group of fluorescein or its analogue is known as the photoswitch as its acylation would quench the fluorescence while acyl deprotection would restore fluorescence [22–27]. With the target molecule, e.g. SBTP-1, we could evaluate this template's sensitivity and specificity to thiols using readily available and sensitive fluorescence spectroscopy. The preparation of SBTP-1 is shown in Scheme 2. Briefly, conjugation between MSBT and thiosalicyclic acid under basic conditions produced compound **1**, which was then subjected to oxidation and esterification with fluorescein to furnish SBTP-1. To study the effects of linker on the sensitivity of the template, we also prepared another fluorescein-based compound SBTP-2 using a more flexible and linear linker propionic acid. SBTP-2 was similarly synthesized from thiol-alkylation between 2-marcaptobenzothiazole and 3-bromoproponic acid followed by oxidation and esterification.

3.2. Fluorescence measurement

With SBTP-1 and SBTP-2 in hand, we tested their fluorescence responses to thiols. As shown in Fig. 1, these two compounds appeared to be stable in buffers. They did not show obvious fluorescence changes if thiols were absent. When they were treated with thiols (GSH, Cys, and Hcy), time- and concentration-dependent fluorescence increases were observed. We also noticed that SBTP-1 (10 μM) reacted more quickly, with the fluorescence emission reaching a maximum steady state in 30 min with 1 mM GSH. In comparison at 60 min SBTP-2 showed very little fluorescent enhancement. These results suggested that benzoic acid was a better linker to facilitate the intramolecular cyclization and the release of the payload.

Because SBTP-1 showed better reactivity to thiols than SBTP-2, we then carefully examined the selectivity of SBTP-1. It was found that SBTP-1 did not respond to other reactive sulfur species such as disulfide and sulfite. It also did not respond to hydrogen peroxide and hypochlorite (Fig. 2A). We further tested SBTP-1 in the presence of representative amino acids (Fig. 2B). These species (alanine, lysine, histidine, tryptophan, arginine, serine, leucine, and tyrosine) did not turn on the fluorescence and they did not affect the effects of thiols on SBTP-1 neither.

To further demonstrate thiol concentration dependence for the release of the payload SBTP-1 was tested with varying GSH concentrations from 0 μM to 100 μM (Fig. 3) The fluorescent intensity was shown to increase with increasing concentrations of GSH demonstrating that the release of the payload was dependent on the thiol concentration.

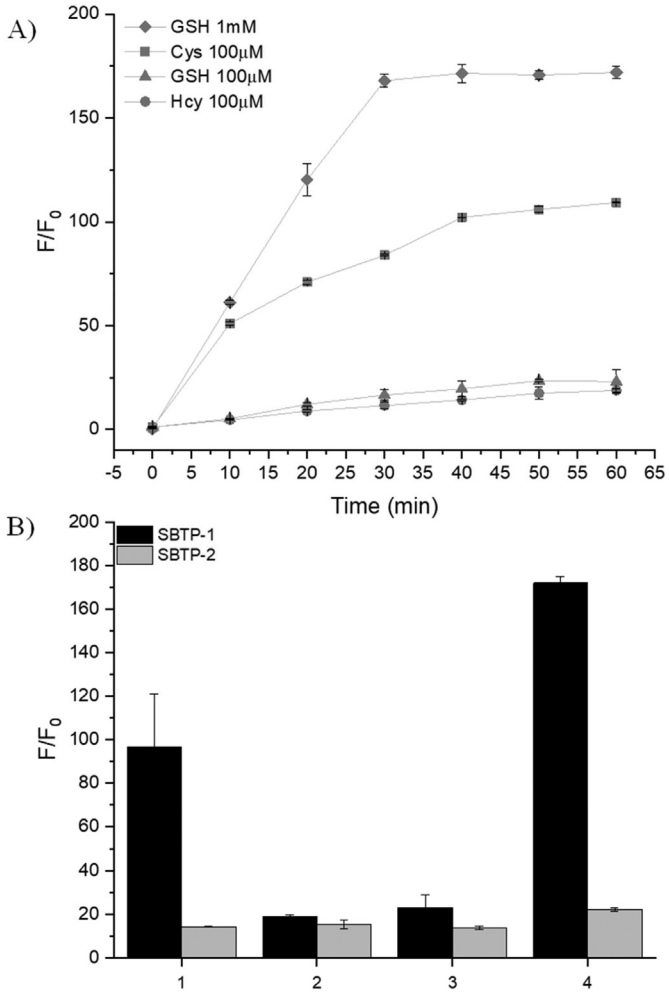

Fig. 1. (A) Time-dependent fluorescence enhancement (F/F_0) of 10 μM SBTP-1 to different biothiols: 100 μM Cys; 100 μM Hcy; 100 μM GSH; and 1 mM GSH. (B) Fluorescence enhancement (F/F_0) of 10 μM probes to different biothiols in 60 min: (1) 100 μM Cys; (2) 100 μM Hcy; (3) 100 μM GSH; (4) 1 mM GSH. The reactions were carried out at 37 °C in PBS buffer (10 mM, pH 7.4) with 50% DMSO.

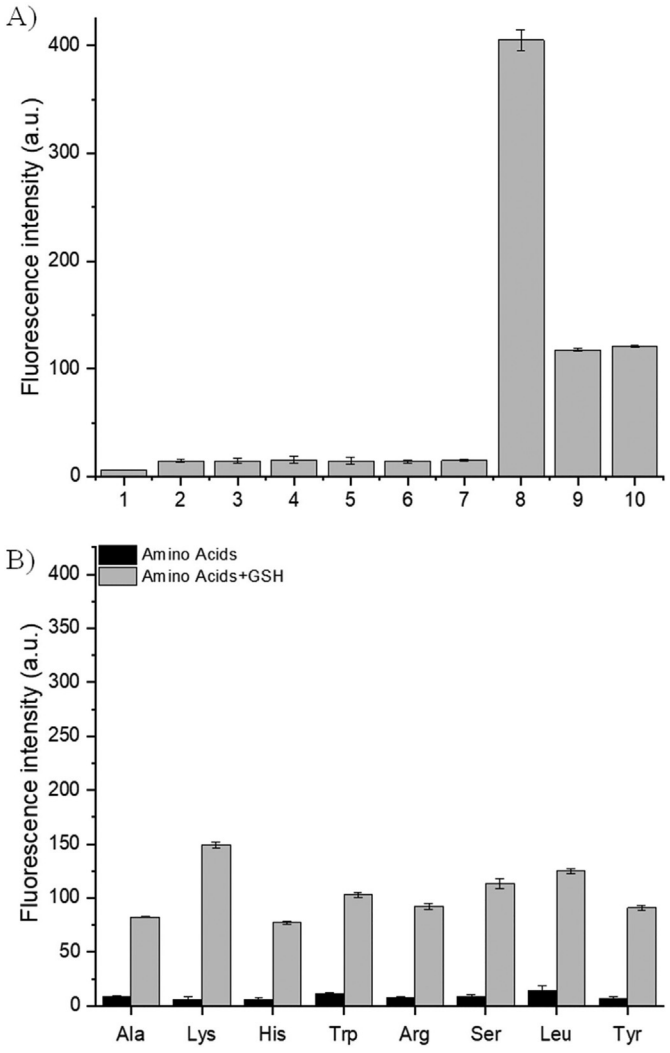

Fig. 2. (A) Fluorescence measurement of SBTP-1 (10 μM) to common oxidants and various RSS: (1) probe alone; (2) 100 μM NaClO; (3) 100 μM H_2O_2; (4) 100 μM $NaNO_2$; (5) 100 μM Na_2SO_3; (6) 100 μM $Na_2S_2O_3$; (7) 100 μM GSSG; (8) 100 μM Cys; (9) 100 μM Hcy; (10) 100 μM GSH. (B) Competitive fluorescence intensity changes of SBTP-1 (10 μM) with and without GSH (100 μM) in the presence of various amino acids (100 μM). All the reactions were carried out for 60 min in PBS buffer (10 mM, pH = 7.4) with 50% DMSO at 37 °C.

We further validated the reaction mechanism of the SBTP sensor by using a model compound SBTP-phenol. The reaction between SBTP-phenol and a cysteine derivative **5** was carried out and the desired product, compound **6**, was obtained in 83% yield, together with phenol and compound **7**. These results confirmed our proposed mechanism (Scheme 3).

3.3. Detection of thiol in plasma

Diseases such as Motor neuron disease, Parkinson's disease, and Alzheimer's disease, show deregulation of plasma thiols, Cys in particular [28]. To demonstrate the practical applicability SBTP-1 was also evaluated in deproteinized fetal bovine serum. As shown in Fig. 4, the reaction of SBTP-1 with thiols can still cause remarkable fluorescence enhancement in deproteinized fetal bovine serum. And a stronger fluorescence was observed after treatment with increasing concentration of Cys. It indicated that SBTP-1 could be used for sensitive detection of biothiols in biological samples.

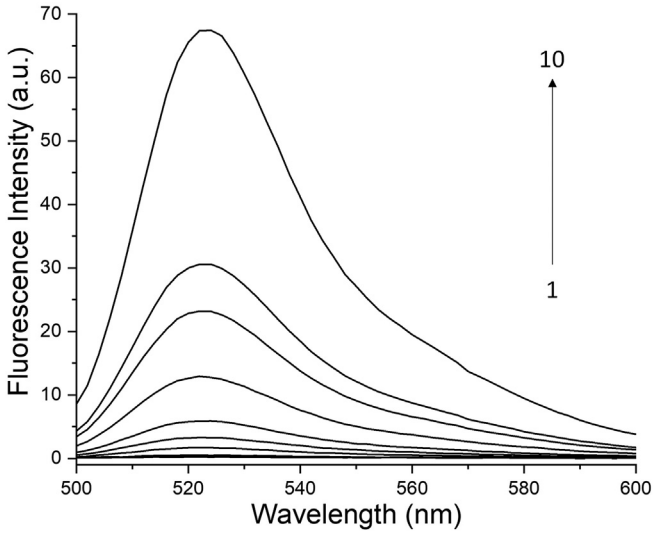

Fig. 3. Fluorescence emission spectra of SBTP-1 (10 μM) with GSH at varied concentrations (0, 1, 5, 10, 15, 20, 30, 40, 50, 100 μM for curves 1–10 respectively). The reactions were carried out for 60 min at 37 °C in PBS buffer (10 mM, pH = 7.4) with 50% DMSO.

3.4. Application in thiol-triggered NO release

All the results with SBTP-1 confirmed that the template was selective and sensitive to thiol-triggering. We next applied this template to prepare a nitric oxide prodrug (e.g. SBTP-NO shown in Scheme 4). *N*-Hydroxy-*N*-nitroso pyrrolidinamine (pyrrolidine-NONOate) was used as the drug payload. It has been previously found that the release NO from another template-furoxans could be mediated by thiol cofactor. Particularly in phenylsulfonyl-substituted furoxans and furoxancarboxamides. Phenylsulfonyl-substituted furoxan has been coupled with anti-cancer drugs for a synergistic effect [29–31]. Our new template provides a versatile tool to expand on thiol-triggered NO release. The synthesis of SBTP-NO started from the esterification of compounds **2** and **8**. The product **9** was then subjected to TBS deprotection, bromination, and alkylation with pyrrolidine-NONOate **11** to afford the prodrug SBTP-NO.

Thiol-triggered NO release from SBTP-NO was then evaluated by using a well-known NO fluorescent probe DAF-2. As shown in Fig. 5, DAF-2 alone, DAF-2 with SBTP-NO, and DAF-2 with GSH (columns 1–3) did not show any fluorescence increase. These indicated that SBTP-NO was stable in testing conditions and not releasing NO on its own. With the authentic NO donor pyrrolidine-NONOate (column 4) we observed strong fluorescence increase. This signal was significantly decreased but still very obvious when GSH was presented (column 5). This could be explained by the competing reaction between NO and GSH that diminished the reaction between NO and DAF-2. Columns 6–8 showed the behavior of SBTP-NO (100 μM) in the presence of thiols. Column 6 contained 1 mM GSH. Similar to the results shown in column 5, while NO release in this sample was obvious, the competing GSH/NO reaction decreased the fluorescence signal. In columns 7 and 8 Cys and Hcy were used at a concentration of 200 μM. This lower concentration of thiol did not have as much of the competing reaction with NO, therefore, fluorescence signal was much stronger. These results demonstrated that thiol indeed could trigger NO release from this template.

4. Conclusion

In summary, we reported herein the discovery of a unique reaction between thiols (RSH) and alkyl sulfonylbenzothiazole. This reaction

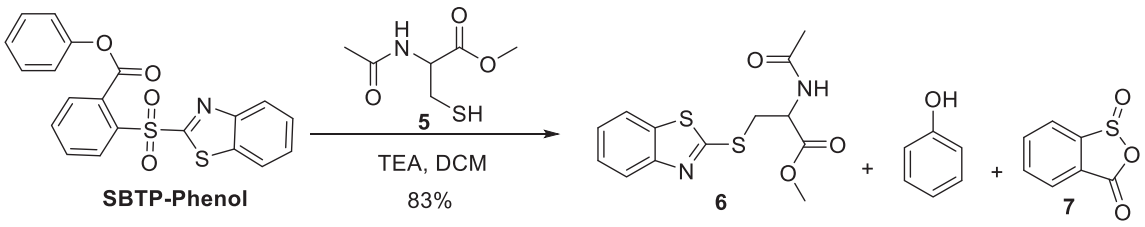

Scheme 3. Model reaction of the sensor with thiols.

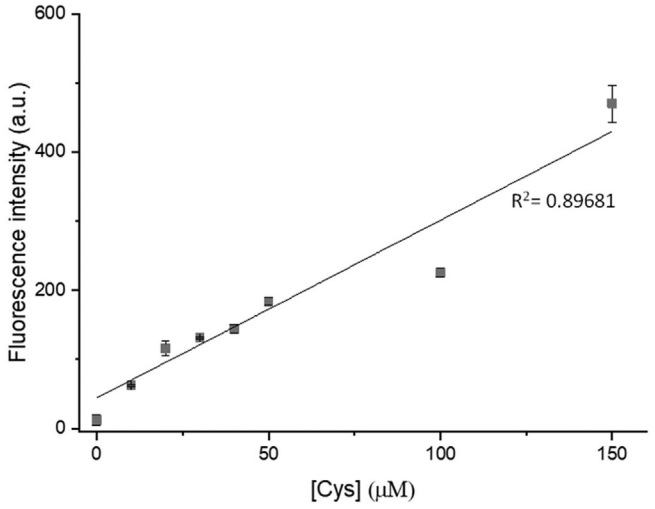

Fig. 4. Fluorescence response of 10 μM SBTP-1 to varied concentrations of Cys in deproteinized fetal bovine serum. The reactions were carried out for 60 min at 37 °C in deproteinized fetal bovine serum with 50% DMSO.

was found to be specific for thiols. Unlike other thiol-specific reactions that normally do not produce reactive intermediates, this reaction produces a sulfinic acid (RSO_2H) as the intermediate, which can further trigger an intramolecular cyclization to release -OH containing payloads. Moreover, the reaction template allows easy modifying all three components: the heterocycle part, the linker, and the payload. As such, it could serve as a modular template for the development of thiol-triggered payload release. This was demonstrated by SBTP-1 (a fluorescent sensor) and SBTP-NO (a NO prodrug). Further optimization of this template and its applications are still undergoing in our lab and will be reported in due course.

CRediT authorship contribution statement

Jessica Renee Knight: Conceptualization, Methodology, Visualization, Investigation. **Yingying Wang:** Methodology, Visualization, Investigation. **Shi Xu:** Methodology, Investigation. **Wei Chen:** Methodology, Writing - review & editing. **Clifford E. Berkman:** Supervision, Writing - review & editing. **Ming Xian:** Conceptualization, Writing - review & editing, Supervision, Funding acquisition.

Declaration of competing interest

There are no conflicts to declare.

Acknowledgement

This work was supported by NSF (CHE1954826) and NIH (GM125968).

Appendix A. Supplementary data

Supplementary data to this article can be found online at https://doi.org/10.1016/j.saa.2020.119072.

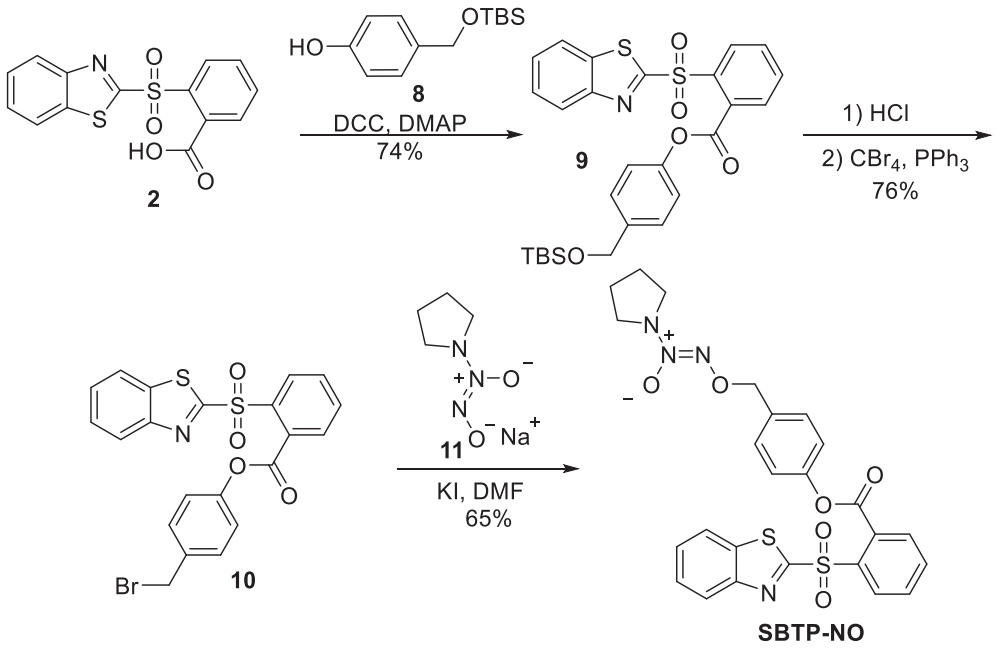

Scheme 4. Synthesis of SBTP-NO.

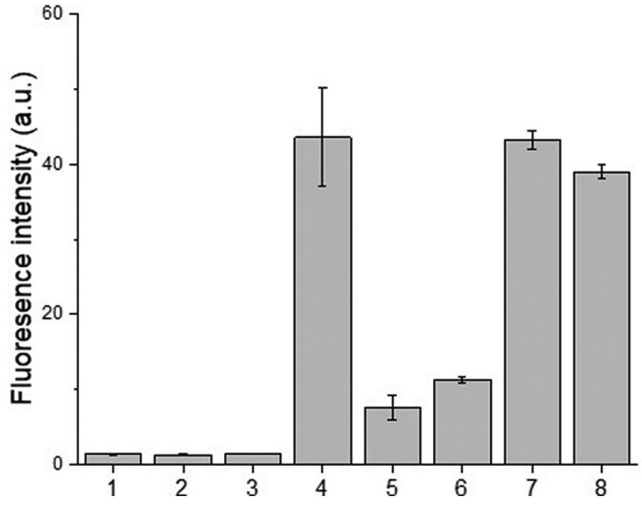

Fig. 5. Fluorescence intensity at of 10 μM DAF-2 in the presence of various reactive species: (1) DAF-2 alone; (2) SBTP-NO (100 μM); (3) GSH (1 mM); (4) pyrrolidine-NONOate (100 μM); (5) GSH (1 mM) and pyrrolidine-NONOate (100 μM); (6) SBTP-NO (100 μM) and GSH (1 mM); (7) SBTP-NO (100 μM) and Cys (200 μM); (8) SBTP-NO (100 μM) and Hcy (200 μM). All the reactions were carried out for 60 min in PBS buffer (10 mM, pH = 7.4) with 50% DMSO at 37 °C.

References

[1] C. Hwang, A.J. Sinskey, H.F. Lodish, Oxidized redox state of glutathione in the endoplasmic reticulum, Science 257 (1992) 1496–1502.

[2] S.A. Lipton, Y.B. Choi, H. Takahashi, D.X. Zhang, W.Z. Li, A. Godzik, L.A. Bankston, Cysteine regulation of protein function – as exemplified by NMDA-receptor modulation, Trends Neurosci. 25 (2002) 474–480.

[3] S.Y. Zhang, C.N. Ong, H.M. Shen, Critical roles of intracellular thiols and calcium in parthenolide-induced apoptosis in human colorectal cancer cells, Cancer Lett. 208 (2004) 143–153.

[4] L.A. Herzenberg, S.C. De Rosa, J.G. Dubs, M. Roederer, M.T. Anderson, S.W. Ela, S.C. Deresinski, L.A. Herzenberg, Glutathione deficiency is associated with impaired survival in HIVdisease, Proc. Natl. Acad. Sci. 94 (1997) 1967–1972.

[5] D.M. Townsend, K.D. Tew, H. Tapiero, The importance of glutathione in human disease, Biomed. Pharmacother. 57 (2003) 145–155.

[6] O. Nekrassova, N.S. Lawrence, R.G. Compton, Analytical determination of homocysteine: a review, Talanta 60 (2003) 1085.

[7] R. Franco, O.J. Schoneveld, A. Pappa, M.I. Panayiotidis, The central role of glutathione in the pathophysiology of human diseases, Arch. Physiol. Biochem. 113 (2007) 234–258.

[8] N. Traverso, R. Ricciarelli, M. Nitti, B. Marengo, A.L. Furfaro, M.A. Pronzato, U.M. Marinari, C. Domenicotti, Role of glutathione in cancer progression and chemoresistance, Oxidative Med. Cell. Longev. 2013 (2013) 972913.

[9] G.K. Balendiran, R. Dabur, D. Fraser, The role of glutathione in cancer, Cell Biochem. Funct. 22 (2004) 343–352.

[10] J.M. Estrela, A. Ortega, E. Obrador, Glutathione in cancer biology and therapy, Crit. Rev. Clin. Lab. Sci. 43 (2006) 143–181.

[11] P. Calvert, K.S. Yao, C. Hamilton, P.J. O'Dwyer, Clinical studies of reversal of drug resistance based on glutathione, Chem. Biol. Interact. 111-112 (1998) 213–224.

[12] K.S. Mani, R. Rajamanikandan, M. Ilanchelian, N. Muralidharan, M. Jothi, S.P. Rajendran, Smart phone assisted quinoline-hemicyanine based fluorescent probe for the selective detection of glutathione and the application in living cells, Spectrochim. Acta A Mol. Biomol. Spectrosc. 243 (2020) 118809.

[13] X. Zhang, H. Liu, Y. Ma, W. Qu, H. He, X. Zhang, S. Wang, Q. Sun, F. Yu, Development of a novel near-infrared fluorescence light-up probe with a large Stokes shift for sensing of cysteine in aqueous solution, living cells and zebrafish, Dyes Pigments 171 (2019) 107722.

[14] M. She, Z. Wang, T. Luo, B. Yin, P. Liu, J. Liu, F. Chen, S. Zhang, J. Li, Fluorescent probes guided by a new practical performance regulation strategy to monitor glutathione in living systems, Chem. Sci. 9 (2018) 8065–8070.

[15] F. Chen, J. Zhang, W. Qu, X. Zhong, H. Liu, J. Ren, H. He, X. Zhang, S. Wang, Development of a novel benzothiadiazole-based fluorescent turn-on probe for highly selective detection of glutathione over cysteine/homocysteine, Sens. Actuators B Chem. 266 (2018) 528–533.

[16] P. Zhou, J. Yao, G. Hu, J. Fang, Naphthalimide scaffold provides versatile platform for selective thiol sensing and protein labeling, ACS Chem. Biol. 11 (2016) 1098–1105.

[17] L.Y. Niu, Y.Z. Chen, H.R. Zheng, L.Z. Wu, C.H. Tung, Q.Z. Yang, Design strategies of fluorescent probes for selective detection among biothiols, Chem. Soc. Rev. 44 (2015) 6143–6160.

[18] H. Peng, W. Chen, Y. Cheng, L. Hakuna, R. Strongin, B. Wang, Thiol reactive probes and chemosensors, Sensors 12 (2012) 15907–15946.

[19] X. Chen, H. Wu, C.-M. Park, T. Poole, G. Keceli, N.O. Devarie-Baez, A.W. Tsang, W.T. Lowther, L.B. Poole, S.B. King, M. Xian, C.M. Furdui, Discovery of heteroaromatic sulfones as a new class of biologically compatible thiol-selective reagents, ACS Chem. Biol. 12 (2017) 2201–2208.

[20] D. Zhang, N.O. Devarie-Baez, Q. Li, J.R. Lancaster, M. Xian, Methylsulfonyl benzothiazole (MSBT): a selective protein thiol blocking reagent, Org. Lett. 14 (13) (2012) 3396–3399.

[21] D. Zhang, W. Chen, J. Kang, Y. Ye, Y. Zhao, M. Xian, Highly selective fluorescence off–on probes for biothiols and imaging in live cells, Org. Biomol. Chem. 12 (2014) 6837–6841.

[22] X. Li, X. Gao, W. Shi, H. Ma, Design strategies for water-soluble small molecular chromogenic and fluorogenic probes, Chem. Rev. 114 (2014) 590–659.

[23] W. Chen, S. Xu, J.J. Day, D. Wang, M. Xian, A general strategy for development of near-infrared fluorescent probes for bioimaging, Angew. Chem. Int. Ed. 56 (2017) 16611–16615.

[24] W. Chen, A. Pacheco, Y. Takano, J.J. Day, K. Hanaoka, M. Xian, A single fluorescent probe to visualize hydrogen sulfide and hydrogen polysulfides with different fluorescence signals, Angew. Chem. Int. Ed. 55 (2016) 9993–9996.

[25] W. Chen, E.W. Rosser, T. Matsunaga, A. Pacheco, T. Akaike, M. Xian, The development of fluorescent probes for visualizing intracellular hydrogen polysulfides, Angew. Chem. Int. Ed. 54 (2015) 13961–13965.

[26] W. Chen, T. Matsunaga, D.L. Neill, C. Yang, T. Akaike, M. Xian, Rational design of a dual-reactivity based fluorescent probe for visualizing intracellular HSNO, Angew. Chem. Int. Ed. 58 (2019) 16067–16070.

[27] J. Sun, Y. Bai, Q. Ma, H. Zhang, M. Wu, C. Wang, M. Tian, A FRET-based ratiometric fluorescent probe for highly selective detection of hydrogen polysulfides based on a coumarin-rhodol derivative, Spectrochim. Acta A Mol. Biomol. Spectrosc. 241 (2020) 118650.

[28] M.T. Heafield, S. Fearn, G.B. Steventon, R.H. Waring, A.C. Williams, S.G. Sturman, Plasma cysteine and sulphate levels in patients with motor neurone, Parkinson's and Alzheimer's disease, Neurosci. Lett. Ed. 110 (1990) 216–220.

[29] M. Feelisch, K. Schönafinger, E. Noack, Thiol-mediated generation of nitric oxide accounts for the vasodilator action of furoxans, Biochem. Pharmacol. 44 (1992) 1149–1157.

[30] G. Sorba, C. Medana, R. Fruttero, C. Cena, A.D. Stilo, U. Galli, A. Gasco, Water soluble furoxan derivatives as NO prodrugs, J. Med. Chem. 40 (1997) 463–469.

[31] Y. Ai, F. Kang, Z. Huang, X. Xue, Y. Lai, S. Peng, J. Tian, Y. Zhang, Synthesis of CDDO–amino acid–nitric oxide donor trihybrids as potential antitumor agents against both drug-sensitive and drug-resistant colon cancer, J. Med. Chem. 58 (2015) 2452–2464.